Kinematic description of wave propagation through a chemical diode

I. Sendiña-Nadal[a)]
Universidad Rey Juan Carlos, Tulipán, s/n. 28933 Móstoles, Spain

M. deCastro[b)] and M. Gómez-Gesteira[c)]
Department of Applied Physics, Faculty of Science, University of Vigo, 32004 Ourense, Spain

The geometry of an active medium can cause wave blocking and induce unidirectional propagation. This well established phenomenon was studied in a previous paper within the framework of the photosensitive Belousov-Zhabotinsky reaction and the associated Oregonator model. In the present paper, as an extension of that study, the main factors that influence this phenomenon are interpreted in terms of a kinematic model. © *2006 American Institute of Physics*. [DOI: 10.1063/1.2221530]

Excitable media, like the heart muscle or the Belousov-Zhabotinsky (BZ) chemical reaction, are known to spread out a local excitation in the form of a wave in all directions. The strength of the perturbation needed to initiate a wave depends on the local excitability of the medium. Chemical diode refers to its electronic counterpart where propagation of electrical or chemical waves of activity is possible only in one direction. This asymmetrical propagation is likely to occur when the excitability of the system is not uniform. A heterogeneous distribution of the excitability, as the presence of dead cardiac tissue, is thought to be one of the causes of the onset of wave breakup or blocking responsible for some of the most important heart diseases. Wave propagation through a chemical diode has been modeled by means of a spatial distribution of excitable fields separated by a low excitable gap. Geometrical constraints and thresholds control the wave passage through the gap. We intend to describe the propagation through a chemical diode by using a simple kinematic model. The wave front resulting from a reaction-diffusion system can be mapped to an oriented curve. Once the geometry of the diode and excitability parameters are given, the kinematic model would be able to predict if propagation is allowed or not in both directions.

I. INTRODUCTION

Wave propagation in an active medium can be considered an isotropic process.[1,2] Nevertheless, under certain external conditions it is possible to block wave propagation in one direction and generate a discontinuous wave front usually called spiral, reentry, or vortex.[3–9] Depending on the field of research, the block of a wave in one direction can give rise to a pernicious effect or constitute the basis of a desired phenomenon. From the point of view of cardiology, the formation of discontinuous wave fronts is related to several life-threatening pathologies,[10–13] which have been

widely studied by means of different active media.[14–17] On the other hand, other authors have proposed the use of unidirectional waves in computing systems.[18–20] In these papers, the unidirectional propagation is achieved by means of the diode-like mechanism proposed by Agladze.[21] This mechanism provides new insights to previous studies[7,22,23] related to the use of active media in parallel computation.

Our aim in this paper is to show how the geometrical properties of the medium can control the observed time evolution of a wave front in a medium with neighboring excitable regions: no propagation, unidirectional, and bidirectional propagation. In a previous work[24] we presented a detailed analysis on how unidirectional propagation is affected by the size and excitability of the medium. Here, we use a kinematic approach to describe most of the features exhibited by unidirectional propagation due to an asymmetric spatial distribution of the excitability by decomposing the motion in several effectively separate modes of wave evolution. In Secs. II and III we present experiments and simulations introducing unidirectional propagation in a chemical diode while Sec. IV is devoted to its kinematic description.

II. EXPERIMENT

Experimentally, we use a spatially extended BZ medium catalyzed by the ruthenium (II)-trisbipyridine, $[Ru(bpy)_3^{+2}]$ complex, which is sensitive to visible light[25] thus allowing spatial control of the excitability of the system.[26] The $[Ru(bpy)_3^{+2}]$ complex is immobilized in a silica gel matrix 1 mm thick and bathed in the BZ solution with concentrations given in Fig. 1. The temperature is kept constant at 25 ± 1 °C. White light (190 Whalogen lamp) passes first through a diffusion screen, then reaches the gel, the interference filter (450.6 nm; transmission 56%) and, finally, the video equipment for image recording. The video images are processed through an image-acquisition card and analyzed on a personal computer. An asymmetric spatial distribution of the excitability is produced by projecting onto the gel a computer generated image via 8-bit gray level light. The darker the gray level the more excitable becomes the reaction.

[a)]Electronic mail: irene.sendina@urjc.es
[b)]Electronic mail: mdecastro@uvigo.es
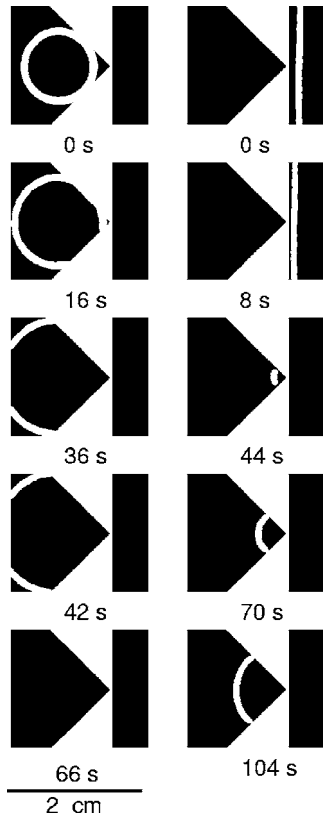[c)]Electronic mail: mggesteira@uvigo.es; URL: http://webs.uvigo.es/ocean

FIG. 1. Experimental diode-like wave propagation in the BZ reaction. Under the same experimental conditions the wave fails to propagate when moving from left to right (CP propagation, left column) and surpasses the gap when propagating from right to left (PC propagation, right column). The dimensions are indicated through the scale bar in the figure, and the light intensity is $107.8\ \mu W/cm^2$. Gel: a solution of 15% sodium silicate, 0.71 mM $[Ru(bpy)_3^{2+}]$, and 0.18 M H_2SO_4; preparation as in Ref. 33. Catalyst-free BZ solution initial concentrations: 0.18 M KBr, 0.33 M malonic acid, 0.39 M $NaBrO_3$, and 0.69 M H_2SO_4.
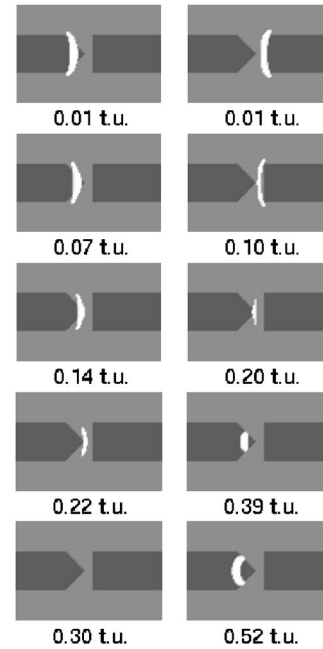

FIG. 2. Numerical diode-like behavior simulated with Eq. (1). For the same model parameters, CP propagation is inhibited (left column) while PC is favored (right column). Parameters of the model: $\varepsilon=0.01$, $f=3$, $q=0.002$, and the values of the parameter ϕ inside and outside the diode are 0.02 and 0.03, respectively. The gap extent is 0.80 s.u. and the channel width 4 s.u.

The excitable field consists of two regions of high excitability, shown as black in Fig. 1, surrounded by a lower excitability area. Dark regions are separated by a small gap (0.9 cm), where the corner C of one region meets the planar side P of the other. Under certain conditions of excitability, the incoming wave propagating from P to C (PC arrangement from now on) is able to surpass the gap (the right column in Fig. 1), but it fails to propagate when moving in the opposite direction (a CP arrangement from now on) (the left column in Fig. 1). This configuration, as first reported in Ref. 21, has been given the name of a chemical diode. Note that the shape of the front arriving at the gap is slightly different in both cases. Although the front curvature can affect propagation through the gap,[24] this fact has little influence on the observed result, since the curvature is negligible in both cases.

III. NUMERICAL RESULT

This experimental phenomenon can be reproduced by performing numerical simulations with the two-variable Oregonator model,[27,28] modified to include the photosensitivity of the BZ reaction:[29]

$$\frac{\partial u}{\partial t} = \frac{1}{\varepsilon}\left(u - u^2 - (fv + \phi)\frac{u-q}{u+q}\right) + D_u \nabla^2 u,$$

$$\frac{\partial v}{\partial t} = u - v,$$

$$(1)$$

where the dimensionless variables u and v correspond to the activator $HBrO_2$ and to the oxidized form of the light-sensitive catalyst $Ru(bpy)_3^{+3}$ concentrations, respectively. $D_u=1$ is the diffusion coefficient of the activator. Since the catalyst is bound to the silica gel medium, there is no corresponding diffusion term for v. The parameter ϕ accounts for the light-induced production of Br^-, which is directly proportional to the light intensity such that the excitability and wave velocity decrease with increasing ϕ. The system given by Eq. (1) is numerically integrated using an Euler method with a time step $\Delta t=10^{-3}$ t.u. and a grid size $\Delta s=0.16$ s.u. in a lattice of 95×65 grid points with zero flux boundary conditions. The Laplacian operator is solved by following a five-point scheme.

The same diode-like behavior previously described in the experiment is observed in numerical simulations as shown in Fig. 2: Successful propagation through the gap for the PC geometrical arrangement (right column), and propagation failure for the CP one (left column). Both numerical experiments are carried out, keeping the same model parameters and geometry of the medium, but changing the initial condition for the propagating direction of the wave.

Figure 3 shows how propagation thresholds for PC and CP arrangements change as a function of the gap extent and of the parameter ϕ outside the diode while keeping constant $\phi=0.02$ inside. One can observe how for the PC arrange-
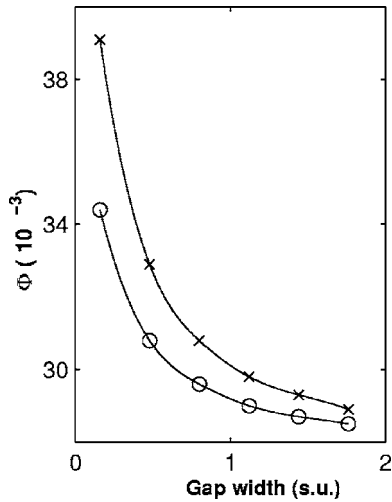
FIG. 3. Curves indicate the limit for propagation through the gap for different gap distances and excitability parameter ϕ values outside the diode. The parameter space where PC propagation is possible (area below the curve with × markers) is bigger than for CP (below the curve with ○ markers).

ment, propagation succeeds in crossing the gap for even higher values of ϕ outside (which means lower excitability) than for the CP one. It can also be observed that for longer gaps propagation fails in both directions, PC and CP, even for higher values of the excitability through the gap.

IV. KINEMATIC DESCRIPTION

This asymmetric propagation can be explained by means of a simple kinematic model,[1,2] which, in turn, only depends on phenomenological parameters: The normal velocity of the wave front at its leading part and the normal and tangential velocities of the wave front at its free ends (see Fig. 4). Considering that the wave front can be mapped to an ori-
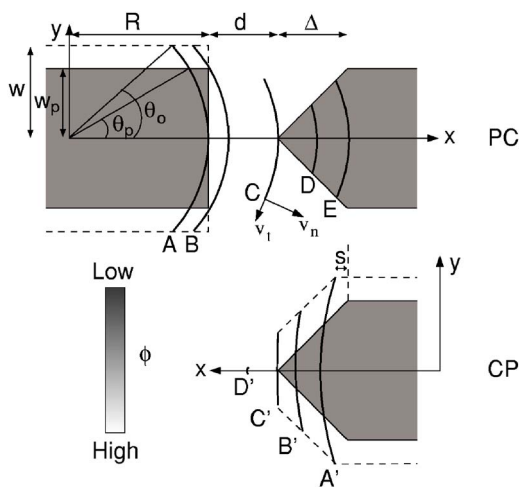

FIG. 4. A sketch of the PC (top) and CP (bottom) propagation. Darker regions have lower excitability parameter ϕ values as indicated by the gray bar. The geometrical parameters as well as the x and y axes used in the kinematic description are shown for each case. A new propagation mode is defined each time there is a change in any of the v_m, v_t, and v_n velocities as the front propagates through the geometrical arrangement of the diode. The dashed lines account for the lateral diffusion length of the activator (the sketch is not to scale, it is just for illustrative purposes). Here $R=4.7$, $d=0.88$, $\Delta=2$, $w=2.48$, $w_p=2$, $s=0.36$, all quantities are in s.u.

ented curve,[1,2] we will assume the following facts: (i) the leading edge of the curve advances with velocity v_m, which adapts instantaneously to the excitability of the medium at the leading point;[30,31] (ii) each small segment of the curve moves in its normal direction with velocity v_n, and the endpoints have a tangential velocity component v_t. These velocities also depend on the instantaneous excitability of the medium at each single point. This instantaneous dependence of the velocity on the excitability is completely fulfilled by v_m and v_t while v_n adapts more slowly but within a spatial scale negligible compared to the rest of the spatial scales involved in the propagation;[30] (iii) despite the front length varies in time, the front shape remains constant. The front is fitted to a circle arc whose center moves at v_m along the x direction and whose radius, R, and curvature, $\kappa=1/R$, are constant; (iv) curvature effect on normal propagation is considered negligible compared to the planar wave front velocity, V_0, since only extreme curvatures can modify propagation.[2,8]

If we consider an expression for the total length, l, of the curve evolving in time:[1,2]

$$\frac{dl}{dt} = \int_o^l \kappa v_n \, ds + 2v_t, \tag{2}$$

the first term describes the elongation of the curve in its normal expansion whereas the second one accounts for the changes in length due to tangential motion of the endpoints of the curve. Integrating Eq. (2) under the assumption κ =const, results in the following temporal variation for the total length:

$$l(t) = (l_0 - l_c)e^{t/\tau} + l_c, \tag{3}$$

where $l_0=l(0)$ is the initial length of the curve, $\tau=(\kappa v_n)^{-1}$ is a characteristic time scale, and $l_c=-2v_t\tau$ is the critical length such that when $l_0>l_c$, $l(t)\to\infty$, and when $l_0<l_c$, $l(t)\to0$.

Observations suggest that propagation under a spatially modulated excitability in a case where the wave surpasses the gap (PC) can be modeled as sketched in the top of Fig. 4. Different propagation modes can be established depending on the front position. Each mode is characterized by a set of v_n, v_t, and v_m parameters whose values depend on the regions the leading part and endpoints are passing through, inside $\{v_n^{\text{in}}, v_t^{\text{in}}, v_m^{\text{in}}\}$ and outside $\{v_n^{\text{out}}, v_t^{\text{out}}, v_m^{\text{out}}\}$ the diode, respectively. At a time t, $l(t)$ is the total length of the front and the Cartesian coordinates of the front points are $x(t,l_f)$, $y(t,l_f)$, where $l_f \in [-l(t)/2, \, l(t)/2]$.

From left to right in Fig. 4, the front advances at v_n^{in}, v_t^{in} and v_m^{in} with a stationary shape and length up to position A. This position will be considered as the initial condition. From A to B the front remains constant in shape and length, but the leading edge starts to propagate at v_m^{out} outside the diode. This first mode evolves from $t=0$ to $t=t_1$ and is characterized by $v_{n1}=v_n^{\text{in}}$, $v_{t1}=v_t^{\text{in}}$ and $v_{m1}=v_m^{\text{out}}$:

$$l(t) = l_0 \quad \text{if } t \leq t_1,$$

$$x(t, l_f) = v_{m1}t + R\cos\left(\frac{l_f}{R}\right), \quad y(t, l_f) = R\sin\left(\frac{l_f}{R}\right), \tag{4}$$

where $l_0 = 2R\theta_0$ is the total initial length of the curve as a function of the angle $\theta_0 = \arcsin(w/R)$ determined by the curve from its center up to one of its endpoints. Time t_1 fulfills the condition $x(t_1, l_p = \theta_p R) = R$ being $\theta_p = \arcsin(w_p/R)$. After solving this condition, $t_1 = R/v_{m1}(1 - \cos\theta_p)$.

From B to C the front is completely outside the region defined by the diode. The leading edge advances at $v_{m2} = v_m^{out}$ and the endpoints contract at $v_{n2} = v_n^{out}$ and $v_{t2} = v_t^{out}$. This second mode is characterized by

$$l(t) = [l(t_1) - l_{c2}]e^{(t-t_1)/\tau_2} + l_{c2} \quad \text{if } t_1 < t \leq t_2,$$

$$x(t, l_f) = x(t_1, 0) - R + R\cos\left(\frac{l_f}{R}\right), \tag{5}$$

$$y(t, l_f) = R\sin\left(\frac{l_f}{R}\right),$$

being $t_2 = d/v_{m2} + t_1(1 - v_{m1}/v_{m2})$ the time the front needs to reach point C, the vertex of the diode, propagating at speed v_{m2}. Note that both l_{c2} and τ_2 depend on v_{t2} and v_{n2}.

From C to D the front still contracts at v_n^{out} and v_t^{out}, but the leading edge moves at $v_{m3} = v_m^{in}$. This third mode is characterized by

$$l(t) = [l(t_2) - l_{c3}]e^{(t-t_2)/\tau_3} + l_{c3} \quad \text{if } t_2 < t \leq t_3,$$

$$x(t, l_f) = x(t_2, 0) - R + v_{m3}(t - t_2) + R\cos\left(\frac{l_f}{R}\right), \tag{6}$$

$$y(t, l_f) = R\sin\left(\frac{l_f}{R}\right),$$

where t_3 is given by the implicit equation $R^2\sin[l(t_3)] + [v_{m3}(t_3 - t_2)]^2 - 2Rv_{m3}(t_3 - t_2) = 0$, which has to be numerically solved. This equation comes from imposing the front at its end points intersects the border of the diode, that is, $y[t_3, l(t_3)/2] = x[t_3, l(t_3)/2] - (R+d)$.

Finally, from E forward the front advances at $v_{m4} = v_m^{in}$ and the free ends expand at $v_{n4} = v_n^{in}$ and $v_{t4} = v_t^{in}$. This growing is limited by the medium extent, in such a way that the front cannot surpass the border of the diode. This last mode is characterized by

$$l(t) = \min[l_m(t), l'(t)] \quad \text{if } t > t_3,$$

$$x(t, l_f) = x(t_3, 0) - R + v_{m4}(t - t_3) + R\cos\left(\frac{l_f}{R}\right), \tag{7}$$

$$y(t, l_f) = R\sin\left(\frac{l_f}{R}\right),$$

where $l'(t) = [l(t_3) - l_{c4}]e^{(t-t_3)/\tau_4} + l_{c4}$ represents the front growth and $l_m(t) = R\arcsin(1 - \{[R - v_{m3}(t_3 - t_2)$
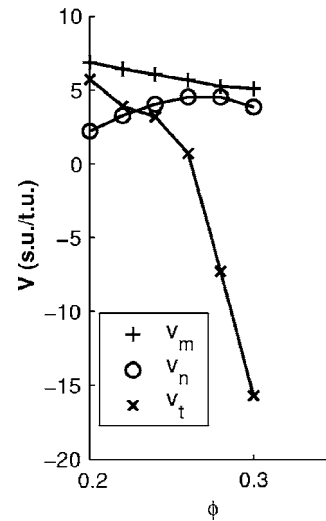

FIG. 5. Propagation velocities (v_m, v_n, and v_t) corresponding to an initially planar wave front in a uniform medium as a function of the excitability ϕ.

$-v_{m4}(t - t_3)]/R\}^2)$ is the maximum front expansion allowed by the medium.

In order to apply this kinematic description to the numerical simulations, the empirical parameters of the model for the different propagation modes have to be obtained. All those parameters are related to the velocities v_m, v_n, and v_t. These are measured by creating an initially planar wave front (2.4 s.u. in length), propagating in a 15.2 s.u. × 10.4 s.u. uniform medium for a given value of the excitability parameter ϕ. The normal and tangential velocities are shown in Fig. 5 as a function of the excitability of the medium. Note that v_m velocity cannot be considered directly from this experiment since in the diode-like arrangement the front propagates through a nonuniform medium (from C to D, part of the front is inside the diode while part is still outside with lower excitability). In fact, when considering a high excitability track surrounded by a low excitability medium, the propagation velocity is strongly dependent on the track width, at least for narrow tracks (see Fig. 6).

Considering the different propagation modes previously defined by Eqs. (4)–(7), the numerical experiment for a PC configuration can be fitted to the kinematic model. The agreement is quite good, at least qualitatively, as shown in Fig. 7, where the temporal evolution of the kinematic front (black thin line) fits the numerical wave front (white shaded) during propagation through and beyond the gap. Quantitatively, in terms of the wave front length,[32] the agreement depends on both the chosen threshold to obtain the binary representation of the numerical wave front ($u \geq 0.3$) and the chosen set of empirical kinematic parameters to adjust the model. In any case, the length given by Eqs. (4)–(7) follows closely the length of the wave front given by the reaction-diffusion equations (1), as shown in the last frame of the figure.

Analogously, propagation in the opposite direction, could be modeled by defining similar independent propagation modes as sketched in the bottom of Fig. 4. In this case we have that, from right to left, the front propagates at v_{m1}
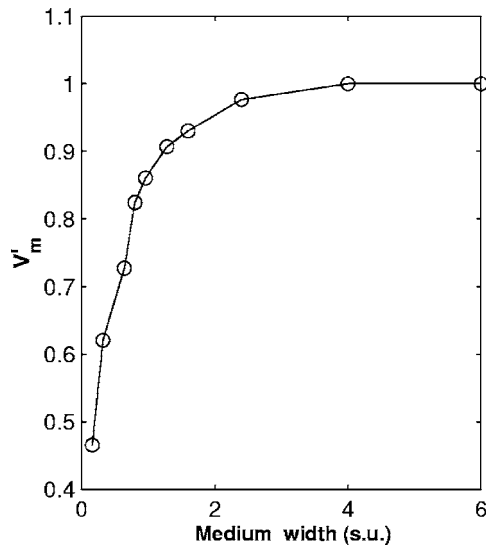
FIG. 6. Dependence of the propagation velocity v_m on the medium width with respect to the maximum value can be attained. Numerical experiments correspond to an initially planar wave front propagating in a rectangular medium of excitability $\phi=0.02$ surrounded by a medium of lower excitability $\phi=0.03$.

$=v_m^{in}$, $v_{n1}=v_n^{out}$, $v_{t1}=v_t^{out}$, contracting at its ends from position A' until it reaches the border at position B':

$$l(t) = (l_0 - l_{c1})e^{t/\tau_1} + l_{c1} \quad \text{if } t \leq t_1,$$

$$x(t,l_f) = R(1 - \cos \theta_0) + s + v_{m1}t + R \cos\left(\frac{l_f}{R}\right), \quad (8)$$

$$y(t,l_f) = R \sin\left(\frac{l_f}{R}\right),$$

where t_1 obeys the expression $\sin[l(t_1)/R](R^2+1)-[R+w-R(1-\cos \theta_0)-v_{m1}t_1]^2=0$ coming from the condition $y[t_1,l(t_1)/2]=-x[t_1,l(t_1)/2]+R+w+s$.

From B' to C', the front will propagate attached to the border following its geometry. This mode is described by

$$l(t) = \max[l_m(t),l'(t)] \quad \text{if } t_1 < t \leq t_2,$$

$$x(t,l_f) = x(t_1,0) - R + v_{m2}(t - t_1) + R \cos\left(\frac{l_f}{R}\right), \quad (9)$$

$$y(t,l_f) = R \sin\left(\frac{l_f}{R}\right),$$

where $l'(t)=[l(t_1)-l_{c2}]e^{(t-t_1)/\tau_2}+l_{c2}$ in this case represents the front decrease and $l_m(t)=R \arcsin(\{[w+R \cos \theta_0-v_{m1}t_1-v_{m2}(t-t_1)]/R\}^2-1)$ is the maximum front expansion allowed by the medium. The time t_2 is given by $t_2=t_1+[\Delta-R(1-\cos \theta_0)-s-v_{m1}t_1]/v_{m2}$, which represents the time the front needs to reach the corner, that is, the solution to the condition $y(t_2,0)=R+\Delta$.

Finally, from position C' to D', the evolution of the front takes place through the region outside the diode, propagating at $v_{m3}=v_m^{out}$ at the leading part and contracting at $v_{n3}=v_n^{out}$ and $v_{t3}=v_t^{out}$ at the endpoints:

$$l(t) = [l(t_2) - l_{c3}]e^{(t-t_2)/\tau_3} + l_{c3} \quad \text{if } t_2 < t \leq t_3,$$

$$x(t,l_f) = x(t_2,0) - R + v_{m3}(t - t_3) + R \cos\left(\frac{l_f}{R}\right), \quad (10)$$

$$y(t,l_f) = R \sin\left(\frac{l_f}{R}\right),$$

where $t_3=t_2+\tau_3\ln[l_{c3}-l(t_2)]$, and is such that $l(t_3)=0$.

Figure 8 shows the numerical evolution of the front (white shaded) through the CP geometrical arrangement superimposed to the analytical front evolution (black thin line) given by Eqs. (8)–(10). Again, it is worth noting the qualitative agreement between the numerical and analytical descriptions. This time the kinematic evolution gives a total length
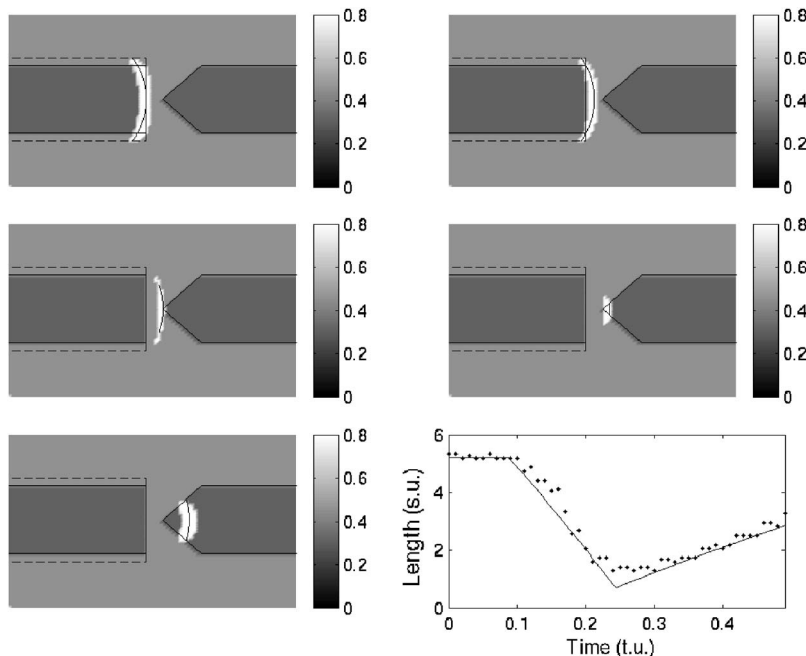

FIG. 7. A comparison between kinematic model results (black thin line) and the numerical experiment (white shaded) for PC propagation. Numerical parameters are the same as in Fig. 2. The graph shows the comparison between the length of the numerical wave front (points) and the length given by the kinematic model (solid line) during time evolution.
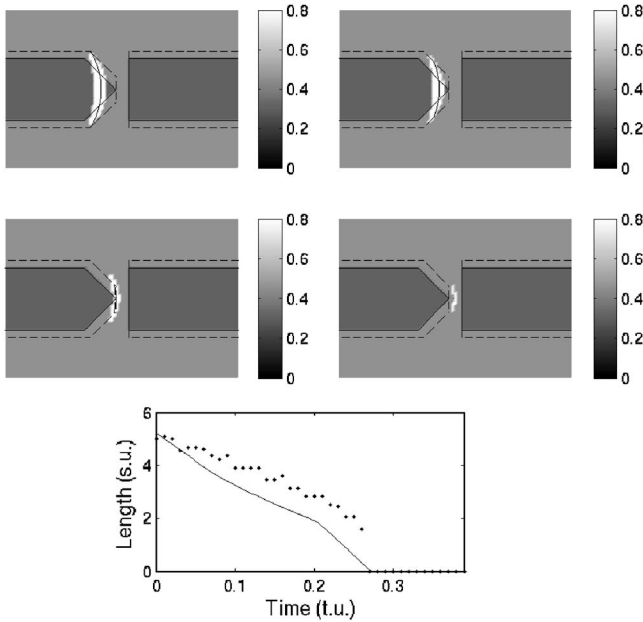
FIG. 8. A comparison between kinematic model results (black thin line) and the numerical experiment (white shaded) for CP propagation. Numerical parameters are the same as in Fig. 2. The graph shows the comparison between the length of the numerical wave front (points) and the length given by the kinematic model (solid line) during time evolution.

of the front below the corresponding numerical value, but it is able to capture the point where the front disappears. The slight disagreement is due to the dependence of the normal velocity on the medium size being a critical factor in this case for CP propagation.

V. CONCLUSIONS

In summary, we have found that a kinematic description for unidirectional propagation in active excitable fields in the presence of a gap between them gives satisfactory results. This description is based on the decomposition of the motion of the wave front in a few independent modes depending on the front position and geometry of the diode-like excitable medium. These modes are simply characterized by a set of empirical velocities at the leading part and at its free ends corresponding just to the propagation through a uniform medium. The presented kinematic description could be extended to other media provided the geometry and the heterogeneous distribution of excitability are known. Thus, the model will allow predicting the fate of a propagating front (bidirectional and unidirectional propagation and blocking) depending on its incident direction. This can be of special interest in the design of computing systems as described in the literature.[18–20]

[1] A. S. Mikhailov, *Foundations of Synergetics. I: Distributed Active Systems* (Springer-Verlag, Berlin, 1991).
[2] V. S. Zykov, *Simulation of Wave Processes in Excitable Media* (Manchester University Press, Manchester, 1987).
[3] M. S. Spach, W. T. Miller, D. Geselowitz, R. C. Barr, J. M. Kootsey, and E. A. Johnson, Circ. Res. **48**, 39 (1981).
[4] M. Gómez-Gesteira, G. Fernández-García, A. P. Muñuzuri, V. Pérez-Muñuzuri, V. I. Krinsky, C. F. Starmer, and V. Pérez-Villar, Physica D **76**, 359 (1994).
[5] J. Starobin, Y. I. Zilberter, and C. F. Starmer, Physica D **70**, 321 (1994).
[6] K. Agladze, J. P. Keener, S. C. Müller, and A. Panfilov, Science **269**, 1857 (1995).
[7] O. Steinbock, P. Kettunen, and K. Showalter, Science **269**, 1857 (1995).
[8] M. Gómez-Gesteira, J. L. del Castillo, M. E. Vázquez-Iglesias, V. Pérez-Muñuzuri, and V. Pérez-Villar, Phys. Rev. E **50**, 4646 (1994).
[9] J. M. Starobin and C. F. Starmer, Phys. Rev. E **54**, 430 (1996).
[10] M. S. Spach, W. T. Miller, P. C. Dolber, J. M. Kootsey, J. R. Sommer, and C. E. Mosher, Circ. Res. **50**, 175 (1982).
[11] A. Kadish, M. Shinnar, E. N. Moore, J. H. Levine, C. W. Balke, and J. F. Spear, Circulation **78**, 1478 (1988).
[12] J. Brugada, L. Boersma, C. Kirchhof, and M. Allessie, Rev. Esp. Cardiol. **43**, 558 (1990).
[13] G. R. Mines, Trans. R. Soc. Can. **4**, 43 (1914).
[14] M. deCastro, M. Gómez-Gesteira, and V. Pérez-Villar, Phys. Rev. E **57**, 949 (1998).
[15] I. P. Mariño, M. D. Rodriguez, V. Pérez-Muñuzuri, M. Gómez-Gesteira, L. O. Chua, and V. Pérez-Villar, IEEE Trans. Circuits and Syst. **42**, 665 (1995).
[16] M. Gómez-Gesteira, M. deCastro, V. Pérez-Villar, and L. O. Chua, IEEE Trans. Circuits Syst., I: Fundam. Theory Appl. **46**, 495 (1999).
[17] G. Bub, A. Shrier, and L. Glass, Phys. Rev. Lett. **88**, 058101 (2002).
[18] I. Motoike and K. Yoshikawa, Phys. Rev. E **59**, 5354 (1999).
[19] I. N. Motoike, K. Yoshikawa, Y. Iguchi, and S. Nakata, Phys. Rev. E **63**, 036220 (2001).
[20] H. Nagahara, T. Ichino, and K. Yoshikawa, Phys. Rev. E **70**, 036221 (2004).
[21] K. Agladze, R. R. Aliev, T. Yamaguchi, and K. Yoshikawa, J. Phys. Chem. **100**, 13895 (1996).
[22] O. Steinbock and P. Kettunen, Chem. Phys. Lett. **251**, 305 (1996).
[23] R. R. Aliev, J. Phys. Chem. **98**, 3999 (1994).
[24] I. Sendiña-Nadal, M. deCastro, F. Sagués, and M. Gómez-Gesteira, Phys. Rev. E **66**, 016215 (2002).
[25] V. Gáspár, G. Bazsa, and M. T. Beck, Z. Phys. Chem. **264**, 43 (1983).
[26] I. Sendiña-Nadal, D. Roncaglia, D. Vives, V. Pérez-Muñuzuri, M. Gómez-Gesteira, V. Pérez-Villar, J. Echave, J. Casademunt, L. Ramírez-Piscina, and F. Sagués, Phys. Rev. E **58**, R1183 (1998).
[27] R. Field and R. Noyes, J. Chem. Phys. **60**, 1877 (1973).
[28] J. Tyson and P. Fife, J. Chem. Phys. **73**, 2224 (1980).
[29] H.-J. Krug, L. Pohlmann, and L. Kuhnert, J. Phys. Chem. **94**, 4862 (1990).
[30] I. Sendiña-Nadal, Ph.D. thesis, Universidade de Santiago de Compostela, 2001, available at http://www.escet.urjc.es/~fisica/investigacion/publications/Papers/ISendinaPhDthesis.pdf
[31] I. Sendiña-Nadal, E. Mihaliuk, J. Wang, V. Pérez-Muñuzuri, and K. Showalter, Phys. Rev. Lett. **86**, 1646 (2001).
[32] The length of the wave calculated from Eq. (1) is obtained first locating the maximum of the u field along the direction of propagation and then adding up those points above a threshold chosen to be 0.3 (a perturbation below this value is unable to spread by diffusion).
[33] T. Yamaguchi, L. Kuhnert, Z. Nagy-Ungvaray, S. C. Müller, and B. Hess, J. Phys. Chem. **95**, 5831 (1991).